Weak currents and Z^0 production in left-right–symmetric gauge models

V. Barger

Physics Department, University of Wisconsin, Madison, Wi. 53706

R. J. N. Phillips

Rutherford Laboratory, Chilton, Didcot, Oxon, England

(Received 15 February 1978)

We present the pheomenology of $SU(2)_L \times SU(2)_R \times U(1)_L \times U(1)_R$ gauge models of the weak and electromagnetic interactions in a simple parametric form, based on the eigenvectors of the intermediate-vector-boson mass matrix. The neutral-current interactions are described in general by four angles and three Z^0 masses. For natural extinction of atomic physics parity violation, one Z boson has pure vector couplings, the other two pure axial-vector couplings. Imposing equivalence with the neutrino scattering phenomenology of the Weinberg-Salam model, only one parameter remains; this degree of freedom allows an axial-vector Z boson to have low mass. The observable consequences of a light Z^0 are explored for e^+e^- annihilation, Drell-Yan production of lepton pairs, deep-inelastic lepton scattering by neutral currents, and the anomalous magnetic moment of the muon. A Z mass as low as 30 GeV is compatible with existing measurements; the most stringent present limit is set by the muon magnetic moment. We estimate a $Z_3(30)$ signal would be about 10% of the $\Upsilon(9.5)$ signal in $pp \to \mu^+\mu^-X$ at top CERN ISR energies $\sqrt{s} = 60$ GeV, and that $Z_3(30)$ would give a -13% asymmetry in $e^+e^- \to \mu^+\mu^-$ at top SPEAR energies $\sqrt{s} = 7.5$ GeV.

I. INTRODUCTION

Gauge models of the weak and electromagnetic interactions with left-right symmetry[1-13] allow a natural explanation for the apparent absence of parity violation in atomic physics.[14,15] In these models the interactions and masses of the intermediate vector bosons can be arranged to preserve the predictions of the standard Weinberg-Salam (WS) model for neutrino scattering,[4,5,16] which agree with all present neutrino experiments. (More general neutrino phenomenologies are possible in the left-right–symmetric models, but such additional freedom is unnecessary at present.) The class of models based on the left-right–symmetric gauge group $SU(2)_L \times SU(2)_R \times U(1)_L \times U(1)_R$ have the particularly interesting property that the mass of the lightest neutral intermediate boson Z^0 is essentially a free parameter, even when this equivalence with the WS model in neutrino scattering is satisfied.[12,13] It is interesting to investigate the predictions of this class of theories for the production of a possible light Z^0 in experiments feasible currently or in the near future.

In this paper we present a systematic discussion of $SU(2)_L \times SU(2)_R \times U(1)_L \times U(1)_R$ gauge model predictions. Rather than following the usual approach of introducing vacuum expectation values of Higgs fields to generate an arbitrary intermediate-boson mass matrix, we start with the diagonal mass matrix of the physical states. The remaining arbitrary parameters of the model enter as rotation angles in the diagonalization matrix that relates the physical fields to the primordial fields and the physical currents to the primordial currents.

Requiring the effective Lagrangian for neutrino scattering to be equivalent to that of the WS model constrains the physical masses and one of the rotation angles. The extinction of atomic physics parity violation constrains two more rotation angles. The one remaining degree of freedom allows a range of masses and current couplings; the light-Z^0 possibility[12,13] is particularly interesting.

In discussing the physical consequence of $SU(2)_L \times SU(2)_R \times U(1)_L \times U(1)_R$ models, we specialize to the one-parameter class described above, that satisfies both equivalence with the WS neutrino sector and atomic parity conservation. In these models, one Z boson (Z_1) has pure vector coupling while Z_2 and Z_3 have pure axial-vector couplings: We call these $V^2 + 2A^2$ neutral-current models. Section III describes the predictions of such models for the masses and widths of the Z bosons and for their effects in e^+e^- annihilation, Drell-Yan production of lepton pairs, deep-inelastic lepton scattering, and the muon anomalous magnetic moment. The Z masses are ordered as $0 \leq m_3 \leq m_1 \leq m_2$; the axially coupled Z_3 can be made arbitrarily light. The Z_3 resonance peak in $e^+e^- \to \mu^+\mu^-$ would exceed background by a factor of order 10^3. In Drell-Yan hadroproduction of lepton pairs, the presence of a Z_3 resonance at mass 9.5 GeV would give a peak-to-background ratio of 2×10^3: This is two orders of magnitude higher than the observed $\Upsilon(9.5)$ enhancement (allowing for experimental resolution), so a Z_3 interpretation of this enhancement is excluded. The present Fermilab data in the lepton-pair mass range $m \leq 15$ GeV exclude a Z_3 of mass below 18 GeV, from the size of the resonance tail. In muon deep-inelastic scat-

tering a light Z_3 leads to a difference between μ^+ and μ^- cross sections, that we calculate. The muon anomalous magnetic moment places the most stringent restriction on the mass of Z_3; the discrepancy between the experimental value and calculated electromagnetic contributions, allowing two standard deviations, permits $m_3 \gtrsim 30$ GeV. We estimate that a $Z_3(30)$ signal would be about 0.1 times the $\Upsilon(9.5)$ signal in $pp \to \mu^+\mu^- X$ at top CERN ISR energies $\sqrt{s} = 60$ GeV, also that $Z_3(30)$ would give a -13% asymmetry in $e^+e^- \to \mu^+\mu^-$ at top SPEAR energies $\sqrt{s} = 7.5$ GeV.

II. TRANSFORMATION FROM GAUGE FIELDS TO PHYSICAL STATES

In $SU(2)_L \times SU(2)_R \times U(1)_L \times U(1)_R$ gauge models, the Lagrangian for the interaction between basic gauge fields and fermions is

$$-i\mathcal{L}_{\rm int} = g\vec{J}_{L\mu} \cdot \vec{W}_{L\mu} + g'J'_{L\mu}B_{L\mu} + (L \to R) ,$$

$$\vec{J}_{L\mu} = \sum_{\psi} \overline{\psi}_L \gamma_\mu \vec{I}_L \psi_L ,$$

$$J'_{L\mu} = \sum_{\psi} \tfrac{1}{2}\overline{\psi}_L \gamma_\mu Y_L \psi_L , \tag{1}$$

where the summation is over the fermion doublets (u, d_C), (c, s_C), (ν_e, e^-), (ν_μ, μ^-), etc. In Eq. (1), $\vec{I}_L = \vec{I}_R = \vec{\tau}/2$ and $Y_L = Y_R$ are assumed with $Y = \frac{1}{3}$ for quarks and $Y = -1$ for leptons. After spontaneous symmetry breaking, the physical boson fields with diagonal mass matrix are linear combinations of $\vec{W}_L$, $\vec{W}_R$, B_L, and B_R.

The charged-boson sector is specified by three independent parameters, the two physical masses m_W, $m_{\tilde{W}}$ and a rotation angle ϵ,

$$\begin{bmatrix} W \\ \tilde{W} \end{bmatrix} = \begin{bmatrix} \cos\epsilon & \sin\epsilon \\ -\sin\epsilon & \cos\epsilon \end{bmatrix} \begin{bmatrix} W_L^\pm \\ W_R^\pm \end{bmatrix} . \tag{2}$$

To remain consistent with the established left-handed nature of charged-current phenomena, we require that $m_{\tilde{W}} \gg m_W$, $\epsilon \ll 1$, and

$$m_W^2 = g^2/(8G_F/\sqrt{2}) . \tag{3}$$

The neutral sector of Eq. (1) involves the photon field A and three massive intermediate-boson fields Z_1, Z_2, Z_3. The parameters are the physical masses m_1, m_2, m_3 and four angles that specify the transformation

$$\begin{bmatrix} A \\ Z_1 \\ Z_2 \\ Z_3 \end{bmatrix} = U(\alpha, \beta, \gamma, \theta) \begin{bmatrix} W_L^3 \\ W_R^3 \\ B_L \\ B_R \end{bmatrix} . \tag{4}$$

To construct the matrix U, we first observe that recovery of the electromagnetic Lagrangian $ie\overline{\psi}\gamma_\mu(I_3 + Y/2)\psi A_\mu$ requires

$$A = \sin\theta(W_L^3 + W_R^3)/\sqrt{2} + \cos\theta(B_L + B_R)/\sqrt{2} , \tag{5}$$

with

$$g\sin\theta = g'\cos\theta = \sqrt{2}e . \tag{6}$$

Since the Z, A fields must be mutually orthogonal, the general form of U is

$$U = U_2(\alpha, \beta, \gamma)U_1(\theta) , \tag{7}$$

with

$$U_1(\theta) = \frac{1}{\sqrt{2}} \begin{bmatrix} s_\theta & s_\theta & c_\theta & c_\theta \\ c_\theta & c_\theta & -s_\theta & -s_\theta \\ 1 & -1 & 0 & 0 \\ 0 & 0 & 1 & -1 \end{bmatrix} \tag{8}$$

and

$$U_2(\alpha, \beta, \gamma) = \begin{bmatrix} 1 & 0 & 0 & 0 \\ 0 & c_\alpha & -s_\alpha c_\beta & s_\alpha s_\beta \\ 0 & s_\alpha c_\gamma & c_\alpha c_\beta c_\gamma - s_\beta s_\gamma & -c_\alpha s_\beta c_\gamma - c_\beta s_\gamma \\ 0 & s_\alpha c_\gamma & c_\alpha c_\beta s_\gamma + s_\beta c_\gamma & -c_\alpha s_\beta s_\gamma + c_\beta c_\gamma \end{bmatrix} , \tag{9}$$

where we use the notation $s_\theta = \sin\theta$, $c_\theta = \cos\theta$, $t_\theta = \tan\theta$, etc. The rotation U_1 separates the photon from the Z fields and U_2 specifies an arbitrary rotation through Euler angles α, β, γ in the Z sector.

The weak neutral-current part of the Lagrangian is expressed in the basis of the physical Z states

(suppressing Lorentz indices)

$$-i\mathcal{L}_{\rm int} = 2\left(\frac{G_F}{\sqrt{2}}\right)^{1/2} m_W J_j \tilde{V}_{jk} Z_k , \tag{10}$$

where V is the 3×3 submatrix of Euler angles of Eq. (9) and

$$J_1 = (J_L^3 + J_R^3)c_\theta - (J_L' + J_R')s_\theta t_\theta ,$$

$$J_2 = J_L^3 - J_R^3 , \qquad\qquad\qquad\qquad (11)$$

$$J_3 = (J_L' - J_R')t_\theta .$$

The effective Lagrangian for small-momentum-transfer interactions can therefore be written

$$\mathcal{L}_{\text{eff}} = 2\sqrt{2}\, G_F m_W^2\, J_j \tilde{V}_{jk} m_k^{-2} V_{kl} J_l . \qquad (12)$$

Specializing to neutrino interactions, we have

$$\mathcal{L}_{\text{eff}}^\nu = 2\sqrt{2}\, G_F m_W^2\, (\bar{\nu}_L \gamma_\mu \nu_L) \tilde{K}^\nu \tilde{V} M^{-2} VJ , \qquad (13)$$

where M is the diagonal mass matrix, J is the quark or lepton current vector of Eq. (11), and

$$\tilde{K}^\nu = (c_\theta^{-1}, 1, -t_\theta)/2 . \qquad\qquad (14)$$

The effective Lagrangian for neutrino scattering in the WS model is

$$\mathcal{L}_{\text{eff}}^\nu = \sqrt{2}\, G_F (\bar{\nu}_L \gamma_\mu \nu_L)[(J_L^3 + J_R^3)(1 - 2s_W^2)$$
$$- 2s_W^2 (J_L' + J_R') + (J_L^3 - J_R^3)], \quad (15)$$

where $s_W = \sin\theta_W$. We now investigate the conditions under which Eq. (13) is equivalent to Eq. (15). First, by comparing the structure of the currents in Eq. (15) with those of Eq. (11), we immediately find the necessary condition[6,12,13]

$$\sin^2\theta = 2\sin^2\theta_W . \qquad\qquad (16)$$

This can be satisfied only if $\sin^2\theta_W \leq 0.5$. The remaining conditions can be summarized as

$$m_W^2\, \tilde{K}^\nu\, \tilde{V} M^{-2} V = \tilde{K}_{\text{WS}}^\nu , \qquad (17)$$

where

$$\tilde{K}_{\text{WS}}^\nu = (c_\theta, 1, 0) . \qquad\qquad (18)$$

Hence, for any given rotation angles (α, β, γ) the WS equivalence of Eq. (17) fixes the Z masses uniquely as

$$m_i^2 = m_W^2\, (VK^\nu)_i / (VK_{\text{WS}}^\nu)_i . \qquad (19)$$

Explicitly taking V to be the Euler rotation submatrix from Eq. (9) we obtain

$$\left(\frac{m_1}{m_W}\right)^2 = \frac{(c_\alpha - s_\alpha c_\beta c_\theta - s_\alpha s_\beta s_\theta)}{c_\theta (c_\alpha c_\theta - s_\alpha c_\beta)} , \qquad\qquad (20)$$

$$\left(\frac{m_2}{m_W}\right)^2 = \frac{(s_\alpha c_\gamma + c_\alpha c_\beta c_\gamma c_\theta - s_\beta s_\gamma c_\theta + c_\alpha s_\beta c_\gamma s_\theta + c_\beta s_\gamma s_\theta)}{c_\theta (s_\alpha c_\gamma c_\theta + c_\alpha c_\beta c_\gamma - s_\beta s_\gamma)} , \qquad\qquad (21)$$

$$\left(\frac{m_3}{m_W}\right)^2 = \frac{(s_\alpha s_\gamma + c_\alpha c_\beta s_\gamma c_\theta + s_\beta c_\gamma c_\theta + c_\alpha s_\beta s_\gamma s_\theta - c_\beta c_\gamma s_\theta)}{c_\theta (s_\alpha s_\gamma c_\theta + c_\alpha c_\beta s_\gamma + s_\beta c_\gamma)} . \qquad\qquad (22)$$

Given rotation angles (α, β, γ) the neutral current of Eq. (10) is

$$-i\mathcal{L}_{\text{int}} = 2\left(\frac{G_F}{\sqrt{2}}\right)^{1/2} m_W \{ (J_V^3 c_\alpha c_\theta - J_A^3 s_\alpha c_\beta - J_V' c_\alpha s_\theta t_\theta + J_A' s_\alpha s_\beta t_\theta) Z_1$$
$$+ [J_V^3 s_\alpha c_\gamma c_\theta + J_A^3 (c_\alpha c_\beta c_\gamma - s_\beta s_\gamma) - J_V' s_\alpha c_\gamma s_\theta t_\theta - J_A' (c_\alpha s_\beta c_\gamma + c_\beta s_\gamma) t_\theta] Z_2$$
$$+ [J_V^3 s_\alpha s_\gamma c_\theta + J_A^3 (c_\alpha c_\beta s_\gamma + s_\beta c_\gamma) - J_V' s_\alpha s_\gamma s_\theta t_\theta - J_A' (c_\alpha s_\beta s_\gamma - c_\beta c_\gamma) t_\theta] Z_3 \} , \qquad (23)$$

where J_V and J_A denote the vector and axial-vector components of the current. Writing the Lagrangian in the general form, summed over fermion types α,

$$-i\mathcal{L}_{\text{int}} = \left(\frac{G_F}{\sqrt{2}}\right)^{1/2} m_W \sum_{i\alpha} (g_{Vi}^\alpha \bar{\psi}_\alpha \gamma_\mu \psi_\alpha + g_{Ai}^\alpha \bar{\psi}_\alpha \gamma_\mu \gamma_5 \psi_\alpha) Z_i , \qquad (24)$$

we find the following coefficients from Eq. (23):
For Z_1 field $(i = 1)$,

$$g_V^\nu = c_\alpha / c_\theta , \qquad g_A^\nu = -s_\alpha (c_\beta + s_\beta t_\theta) ,$$

$$g_V^e = -c_\alpha (c_\theta - s_\theta t_\theta) , \qquad g_A^e = s_\alpha (c_\beta - s_\beta t_\theta) ,$$

$$g_V^u = c_\alpha (c_\theta - s_\theta t_\theta / 3) , \qquad g_A^u = -s_\alpha (c_\beta - s_\beta t_\theta / 3) ,$$

$$g_V^d = -c_\alpha (c_\theta + s_\theta t_\theta / 3) , \qquad g_A^d = s_\alpha (c_\beta + s_\beta t_\theta / 3) .$$

For Z_2 field $(i = 2)$,

$$g_V^\nu = s_\alpha c_\gamma / c_\theta , \qquad g_A^\nu = c_\alpha c_\gamma (c_\beta + s_\beta t_\theta) - s_\gamma (s_\beta - c_\beta t_\theta) ,$$

$$g_V^e = -s_\alpha c_\gamma (c_\theta - s_\theta t_\theta) , \qquad g_A^e = -c_\alpha c_\gamma (c_\beta - s_\beta t_\theta) + s_\gamma (s_\beta + c_\beta t_\theta) ,$$

$$g_V^u = s_\alpha c_\gamma (c_\theta - s_\theta t_\theta / 3) , \qquad g_A^u = c_\alpha c_\gamma (c_\beta - s_\beta t_\theta / 3) - s_\gamma (s_\beta + c_\beta t_\theta / 3) ,$$

$$g_V^d = -s_\alpha c_\gamma (c_\theta + s_\theta t_\theta / 3) , \qquad g_A^d = -c_\alpha c_\gamma (c_\beta + s_\beta t_\theta / 3) + s_\gamma (s_\beta - c_\beta t_\theta / 3) .$$

For Z_3 field $(i = 3)$

$$g_V^\nu = s_\alpha s_\gamma / c_\theta \,, \quad g_A^\nu = c_\alpha s_\gamma (c_\beta + s_\beta t_\theta) + c_\gamma (s_\beta - c_\beta t_\theta) \,,$$

$$g_V^e = -s_\alpha s_\gamma (c_\theta - s_\theta t_\theta) \,, \quad g_A^e = -c_\alpha s_\gamma (c_\beta - s_\beta t_\theta) - c_\gamma (s_\beta + c_\beta t_\theta) \,,$$

$$g_V^u = s_\alpha s_\gamma (c_\theta - s_\theta t_\theta / 3) \,, \quad g_A^u = c_\alpha s_\gamma (c_\beta - s_\beta t_\theta / 3) + c_\gamma (s_\beta + c_\beta t_\theta / 3) \,,$$

$$g_V^d = -s_\alpha s_\gamma (c_\theta + s_\theta t_\theta / 3) \,, \quad g_A^d = -c_\alpha s_\gamma (c_\beta + s_\beta t_\theta / 3) - c_\gamma (s_\beta - c_\beta t_\theta / 3) \,.$$

In the above, d denotes the Cabibbo-rotated combination $d_C = d \cos\theta_C + s \sin\theta_C$ and the couplings of other quark and lepton doublets are the same as above, e.g.,

$$g(\nu_e, e) = g(\nu_\mu, \mu) = g(\nu_\tau, \tau) \,,$$

$$g(u, d_C) = g(c, s_C) = g(t, b) \,.$$

To summarize the results of this section, the physics of the $SU(2)_L \times SU(2)_R \times U(1)_L \times U(1)_R$ gauge model is described by the Lagrangian Eq. (24) with three arbitrary Z masses and four arbitrary rotation angles $\alpha, \beta, \gamma, \theta$. To establish equivalence with the neutrino scattering phenomenology of the WS model, the angle θ must be related to θ_W as in Eq. (16), and the three masses are uniquely determined by α, β, γ through Eqs. (20)–(22). The model thereby admits a three-parameter family of solutions.

The extinction of parity violation in atomic physics can be achieved naturally (i.e., without detailed tuning of parameters) in the left-right–symmetric gauge model if one Z field is purely vector, the other two axial vector. The choice $\alpha = 0$ makes Z_1 vector and Z_2, Z_3 axial vector. There then remains one free parameter $\phi \equiv \beta + \gamma$. In the rest of this paper we concentrate attention on this one-parameter class, which we term $V^2 + 2A^2$ neutral-current models. This particular class is equivalent to those considered in Refs. 12, 13.

The freedom to adjust the Z masses as above arises only because there are three Z bosons. In $SU(2)_L \times SU(2)_R \times U(1)$ models[1-11] where there are just two Z bosons, an analysis similar to that above can be made; to establish equivalence with WS neutrino scattering, the masses are fixed in terms of a single rotation angle (in contrast to the three rotation angles α, β, γ). Then the extinction of atomic physics parity violation fixes this remaining degree of freedom, and the Z masses cannot be further adjusted. [In $SU(2) \times U(1) \times U(1)'$ models[15] there is additional freedom, because no left-right symmetry is imposed and the choice of $U(1)'$ representations is very arbitrary; however, parity conservation in atoms is accidental not systematic here.]

III. PREDICTIONS OF $V^2 + 2A^2$ NEUTRAL-CURRENT MODELS

A. Masses and couplings

In this Section we consider $V^2 + 2A^2$ parity-conserving neutral-current models, in which Z_1 has purely vector couplings while Z_2 and Z_3 have purely axial-vector couplings. The masses and coupling coefficients defined in Sec. II take simple forms in terms of the parameters θ and $\phi = \beta + \gamma$. Here θ is constrained by the neutrino data to $\sin^2\theta = 2 \sin^2\theta_W = 0.5-0.7$ and ϕ is a free parameter. The mass formulas are

$$m_W = \left(\frac{\sqrt{2}\,\pi\alpha}{G_F \sin^2\theta} \right)^{1/2} = \frac{52.8 \text{ GeV}}{\sin\theta} \,,$$

$$m_1 = \frac{m_W}{\cos\theta} = \left(\frac{105.6 \text{ GeV}}{\sin 2\theta} \right),$$

$$m_2 = m_W \left(\frac{\cos(\phi - \theta)}{\cos\theta \cos\phi} \right)^{1/2} ,$$

$$m_3 = m_W \left(\frac{\sin(\phi - \theta)}{\cos\theta \sin\phi} \right)^{1/2} .$$

(25)

Hence the allowed range for ϕ is $\theta \le \phi < \pi/2$. We note the mass inequalities,
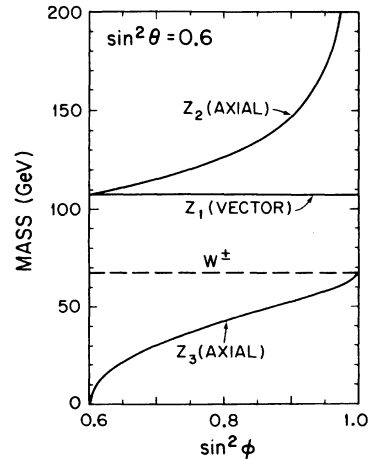

FIG. 1. Dependence of the Z masses on the parameter ϕ, for the choice $\sin^2\theta = 0.6$.

$$0 \leq m_3 \leq m_W < m_1 \leq m_2 . \qquad (26)$$

The possibility of an arbitrarily light Z_3 is particularly interesting.

Figure 1 illustrates the dependence of the Z masses on the parameter ϕ with the choice $\sin^2\theta = 0.6$; for which $m_W = 68$ GeV. Corresponding results are also given in Refs. 12, 13.

The coupling coefficients defined in Sec. II also take simple forms. The Z_1 coefficients are $g_A^\alpha = 0$ and

$$g_V^\nu = 1/c_\theta, \quad g_V^u = c_\theta - s_\theta t_\theta /3 , \qquad (27)$$

$$g_V^e = -c_\theta + s_\theta t_\theta , \quad g_V^d = -c_\theta - s_\theta t_\theta /3 .$$

The Z_2 coefficients are $g_V^\alpha = 0$ and

$$g_A^\nu = c_\phi + s_\phi t_\theta , \quad g_A^u = c_\phi - s_\phi t_\theta /3 , \qquad (28)$$

$$g_A^e = -c_\phi + s_\phi t_\theta , \quad g_A^d = -c_\phi - s_\phi t_\theta /3 .$$

The Z_3 coefficients are $g_V^\alpha = 0$ and

$$g_A^\nu = s_\phi - c_\phi t_\theta , \quad g_A^u = s_\phi + c_\phi t_\theta /3 , \qquad (29)$$

$$g_A^e = -s_\phi - c_\phi t_\theta , \quad g_A^d = -s_\phi + c_\phi t_\theta /3 ,$$

The g^e couplings are especially significant since initial experimental detection of Z bosons will likely be based on $Z \rightarrow e^+ e^-$ or $\mu^+ \mu^-$. We notice that the light Z_3 has a substantial g_A^e, which is not the case for Z_1 or Z_2; in particular g_V^e of Z_1 vanishes identically for $\sin^2\theta = 0.5$.

For comparison, the coupling coefficients in the WS model are $g_A^\nu = -g_A^e = g_A^u = -g_A^d = g_V^\nu$
$= 1/(\sqrt{2}c_W)$, $g_V^e = (-1 + 4 s_W^2)/(\sqrt{2}c_W)$, g_V^u
$= (1 - 8 s_W^2/3)/(\sqrt{2}c_W)$, $g_V^d = (-1 + \frac{4}{3} s_W^2)/(\sqrt{2}c_W)$,
and $m_Z = m_W/c_W$.

B. Decay widths

The partial widths for fermion-antifermion decays are
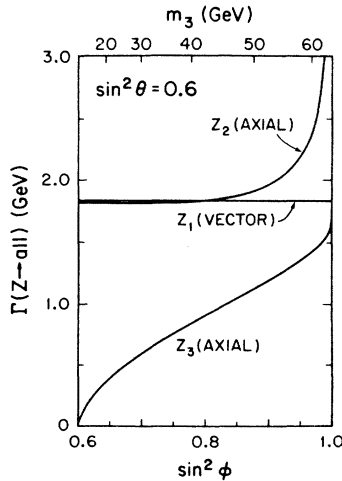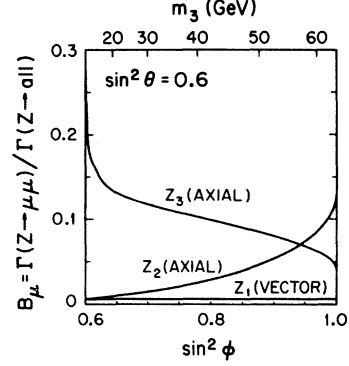
$$\Gamma(Z \rightarrow f\bar{f}) = \frac{m_W^2 m_Z G_F N_c}{24\pi \sqrt{2}} [g_V^2(3\eta - \eta^3) + 2g_A^2\eta^3] , \qquad (30)$$

where $N_c = 1$ for leptons, $N_c = 3$ for quarks, and $\eta = (1 - 4m_f^2/m_Z^2)^{1/2}$. Note that Z decays give rise to both left- and right-handed ν states in left-right–symmetric models. We estimate the widths for six flavors of leptons and quarks, using the mass assignments in GeV units: $m_\tau = 1.85$, $m_{\nu_\tau} = 0$, $m_u = m_d = 0.3$, $m_c = 1.5$, $m_s = 0.5$, $m_t = 6.0$, $m_b = 4.7$. These quark masses are based on $m_u \simeq m_d \simeq m_N/3, m_c \simeq m_\psi/2, m_s \simeq m_K$, and $m_b \simeq m_\Upsilon/2$; the m_t mass is speculation. Figure 2 shows the resulting total widths of the three Z bosons vs $\sin^2\phi$. The branching fractions for $Z \rightarrow \mu^+\mu^-$ and $Z \rightarrow$ hadrons are shown in Figs. 3 and 4. For comparison in the WS model $\Gamma(Z \rightarrow \text{all}) = 1.80$ GeV, $B(Z \rightarrow \mu^+\mu^-) = 0.03$, and $B(Z \rightarrow \text{hadrons}) = 0.70$.
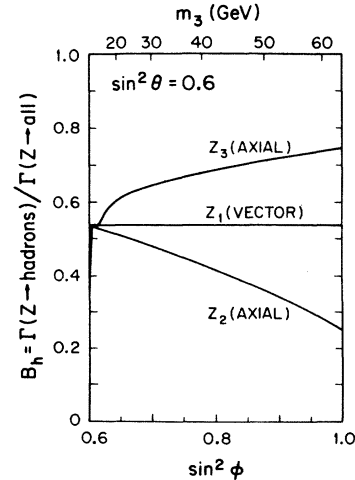

FIG. 2. Total widths of Z bosons vs $\sin^2\phi$, for $\sin^2\theta = 0.6$.

FIG. 4. Branching fractions for $Z \rightarrow$ hadrons.

C. Production by e^+e^- colliding beams

The unpolarized differential cross section for $e^+e^- \to \mu^+\mu^-$ has the form[17]

$$\frac{d\sigma}{dz} = \frac{\pi\alpha^2}{2s}\left\{1+z^2+2\,\mathrm{Re}\left((1+z^2)\sum_i G_{Vi}{}^2+2z\sum_i G_{Ai}{}^2\right)+(1+z^2)\left(\left|\sum_i G_{Vi}\right|^2+\left|\sum_i G_{Ai}\right|^2+2\left|\sum_i G_{Vi}G_{Ai}\right|^2\right)\right.$$

$$\left.+4z\,\mathrm{Re}\left[\left(\sum_i G_{Vi}{}^2\right)\left(\sum_j G_{Aj}{}^{2*}\right)+\left(\sum_i G_{Vi}G_{Ai}\right)\left(\sum_j G_{Vj}^* G_{Aj}^*\right)\right]\right\}, \tag{31}$$

where s is the total c.m. energy squared, z $=\cos\theta_{c.m.}$ (with $\theta_{c.m.}$ defined as the angle of μ^- relative to e^-) and the coefficients G are defined as

$$G_{Vi}{}^2 = \frac{(g_{Vi}^e)^2}{4\sin^2\theta}\,\frac{s}{s-m_i^2+im_i\Gamma_i} \tag{32}$$

and similarly for $V \to A$. Equation (31) includes

both Z-A and Z-Z interferences, but neglects enhancements from hadronic resonances such as ψ.

The integrated cross section is shown vs $\sqrt{s}/m_3$ in Fig. 5, with $\sin^2\theta = 0.6$, for various values of $\sin^2\phi$ corresponding to $m_1 = 20$, 30, 40, 50 GeV. Figure 6 shows the cross section vs $\sqrt{s}$ for $m_3 = 30$ GeV.

At a Z-resonance energy, the ratio of the resonance contribution (peak minus background) to
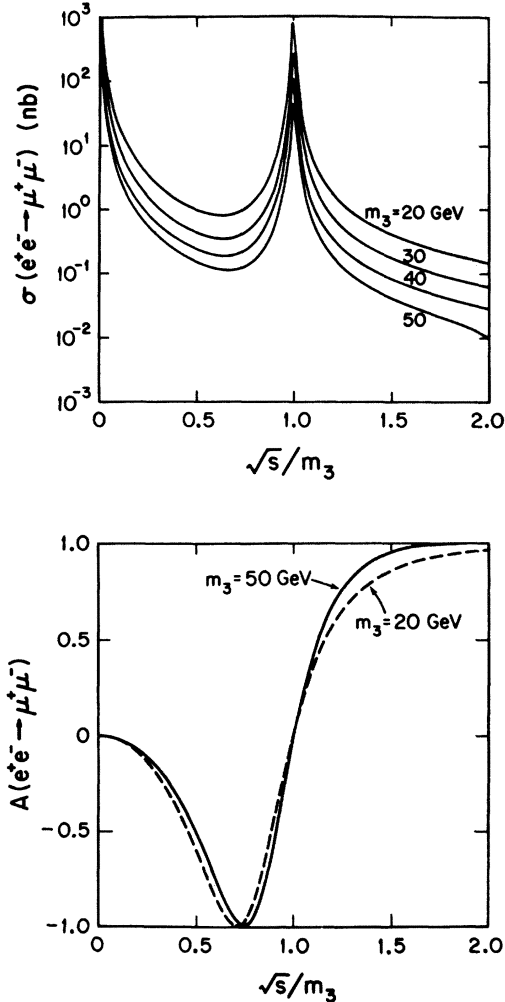
FIG. 5. Total $e^+e^- \to \mu^+\mu^-$ cross section and asymmetry parameter $A(z = 1)$ vs $\sqrt{s}/m_3$. The cases shown have $\sin^2\phi = 0.64$, 0.70, 0.78, 0.88 (with $\sin^2\theta = 0.6$) corresponding to $m_3 = 20$, 30, 40, 50 GeV.

FIG. 6. Total $e^+e^- \to \mu^+\mu^-$ cross section and asymmetry parameter $A(z = 1)$, vs $\sqrt{s}$ for $m_3 = 30$ GeV. The WS-model prediction is shown for comparison.
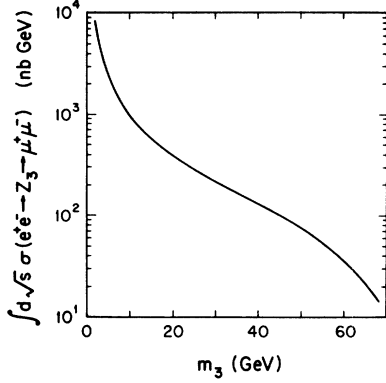
FIG. 7.   Integrated Z_3 resonance contribution $\int d\sqrt{s}\ \delta(e^+e^-\to Z_3\to\mu^+\mu^-)$ vs the mass m_3.

FIG. 8.   Asymmetry parameter $A\,(z=1)$ vs m_3 at $\sqrt{s}=7.5$ GeV.
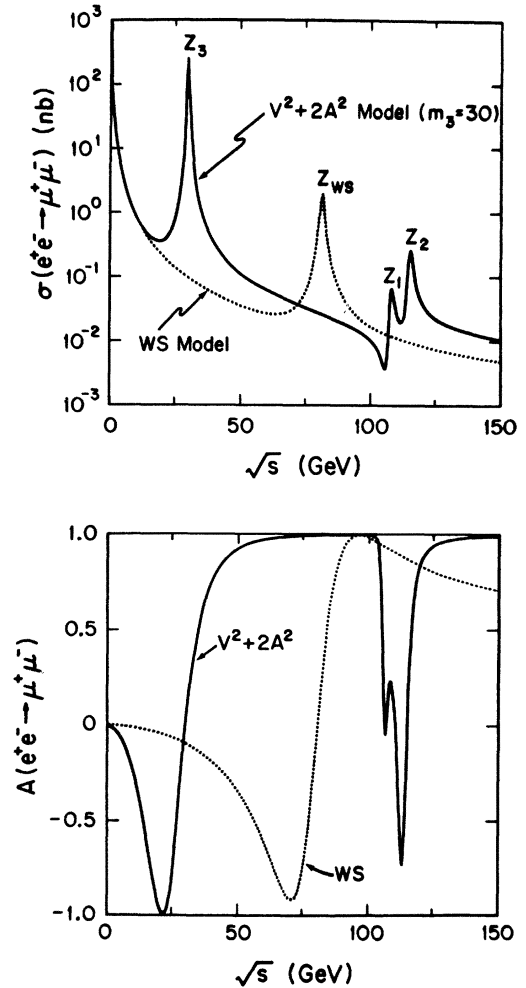
the electromagnetic background is

$$\frac{\sigma(e^+e^-\to Z\to\mu^+\mu^-)}{\sigma(e^+e^-\to\gamma\to\mu^+\mu^-)}=\frac{9}{\alpha^2}B_\mu^2=1.7\times10^5B_\mu^2,\quad(33)$$

$$\frac{\sigma(e^+e^-\to Z\to\text{hadrons})}{\sigma(e^+e^-\to\gamma\to\mu^+\mu^-)}=\frac{9}{\alpha^2}B_\mu B_h,\quad(34)$$

where B_μ is the $Z\to\mu^+\mu^-$ branching fraction and B_h is the $Z\to$ hadrons branching fraction. From the B_μ and B_h values for Z_3 shown in Figs. 3 and 4, the peak-to-background ratios are of order 2×10^3 for $\mu^+\mu^-$ and 1×10^4 for hadrons. The integrated resonance contributions above background are

$$\int d\sqrt{s}\ \sigma(e^+e^-\to Z\to\mu^+\mu^-)=6\pi^2B_\mu^2\Gamma_z/m_z^2,\quad(35)$$

$$\int d\sqrt{s}\ \sigma(e^+e^-\to Z\to\text{hadrons})=6\pi^2B_\mu B_h\Gamma_z/m_z^2.\quad(36)$$

Figure 7 shows the behavior of this integrated contribution for the lightest boson Z_3; we observe that it depends strongly on the mass m_3. We note that Eqs. (31)–(36) apply to any narrow spin-1 resonance.

The forward-backward asymmetry of the differential cross section in Eq. (31) has the form

$$A(z)=\frac{d\sigma(z)-d\sigma(-z)}{d\sigma(z)+d\sigma(-z)}=\frac{2z}{1+z^2}A(z=1).\quad(37)$$

The asymmetry parameter $A(z=1)$ is shown vs $\sqrt{s}/m_3$ in Fig. 5, for $\sin^2\theta=0.6$ with several values of m_3 and in Fig. 6 vs $\sqrt{s}$ for $m_3=30$ GeV. The corresponding prediction of the WS model with $\sin^2\theta_W=0.3$ is shown in Fig. 6 for comparison. The predicted asymmetry for SPEAR at $\sqrt{s}=7.5$ GeV is $A(z=1)=-0.13$ for $m_3=30$ GeV, well within the sensitivity of forthcoming measurements. For a mass $m_3=50$ GeV, the prediction is $A(z=1)=-0.04$. Figure 8 shows $A(z=1)$ vs m_3 at $\sqrt{s}=7.5$ GeV.

The absence of parity-violating amplitudes in the V^2+2A^2 model means that (i) with longitudinally polarized beams, there is no asymmetry between helicity configurations $+1,+1$ and $-1,-1$; (ii) the longitudinal polarization of either final muon vanishes.

We have concentrated our attention here on $\mu^+\mu^-$ and hadron modes; a similar analysis can be made for $e^+e^-\to e^+e^-$, which has different A^2 and Z-A terms.

D. Drell-Yan production

Following the Drell-Yan approach,[18] lepton-pair production in hadron-hadron collisions can be described in terms of a basic quark-antiquark annihilation process, with this sub–cross section given by

$$\sigma(q_k\bar{q}_k\to\mu^+\mu^-)=\frac{4\pi\alpha^2}{3m^2}\Big[e_k^2+2e_k\,\mathrm{Re}\Big(\sum_i G_{Vi}H_{Vi}\Big)+\Big|\sum_i G_{Vi}H_{Vi}\Big|^2+\Big|\sum_i G_{Ai}H_{Ai}\Big|^2$$

$$+\Big|\sum_i G_{Vi}H_{Ai}\Big|^2+\Big|\sum_i G_{Ai}H_{Vi}\Big|^2\Big].\quad(38)$$

Here k labels the quark flavor, e_k is the quark charge, m is the muon pair mass, G_{Vi}, G_{Ai} are as defined in Eq. (32) with $s = m^2$, and

$$H_{Vi}G_{Vi} = \frac{g^e_{Vi}g^q_{Vi}}{4\sin^2\theta} \frac{m^2}{m^2 - m_i^2 + im_i\Gamma_i} , \qquad (39)$$

and similarly for $V \rightarrow A$. In terms of this subcross section, the Drell-Yan formula for $AB \rightarrow \mu^+\mu^-\chi$ inclusive pair production is

$$\frac{d\sigma}{dydm} = \frac{2x_+x_-}{3m} \sum_k f_k^A(x_+)f_k^B(x_-)\sigma(q_kq_{\bar{k}} \rightarrow \mu^+\mu^-) . \qquad (40)$$

Here $f_k^a(x)$ is the fractional momentum distribution of quark k in particle A, f_k^B is defined similarly, the summation runs over all quark and antiquark flavors. Also y is the rapidity of the muon pair, $x_\pm = \exp(\pm y)m/\sqrt{s}$ and $s = (p_A + p_B)^2$ is the c.m. energy squared. Typically, for an arbitrary nucleus $A = (N, Z)$ the u distribution functions are $f_u^A = Zu(x) + Nd(x)$, $f_{\bar{u}}^A = Z\bar{u}(x) + N\bar{d}(x)$; for incident protons $f_u^p = u(x)$, $f_{\bar{u}}^p = \bar{u}(x)$ and for incident anti-protons $f_u^{\bar{p}} = u(x)$, $f_{\bar{u}}^{\bar{p}} = \bar{u}(x)$.

At the μ-pair mass value corresponding to a Z resonance, the ratio of the resonance cross section (peak minus background) to the electromagnetic continuum cross section is

$$\frac{d\sigma(AB \rightarrow ZX \rightarrow \mu^+\mu^-X)/dydm}{d\sigma(AB \rightarrow \gamma X \rightarrow \mu^+\mu^-X)/dydm} = \frac{3}{\alpha^2} B_\mu \bar{B}_q$$

$$\simeq 0.6 \times 10^5 B_\mu \bar{B}_q , \qquad (41)$$

$$\bar{B}_q = \left(\sum_k B_{q_k}f_k^A(x_+)f_k^B(x_-)\right) \Big/ \left(\sum_k e_k^2 f_k^A(x_+)f_k^B(x_-)\right) , \qquad (42)$$

where B_μ, B_{q_k} are the branching rations for $Z \rightarrow \mu^+\mu^-$, $Z \rightarrow q_k\bar{q}_k$ decays, calculated from Eq. (30). Figure 3 shows that B_μ for Z_3 is of order 0.1. Since u and d are the dominant quarks in nuclear targets, $\bar{B}_q$ is essentially determined by the $u\bar{u}$ and $d\bar{d}$ branching ratios.

It is interesting to compare the $\Upsilon(9.5)$ production data[20] with what would be expected from a Z_3 of that mass. For $m_3 = 9.5$ GeV we have

$$\Gamma_3 = 0.14 \text{ GeV} ,$$

$$B_\mu = 0.17 , \qquad (43)$$

$$\bar{B}_q \simeq 0.51 ,$$

from which Eq. (41) yields a peak-to-background ratio

$$d\sigma(Z_3(9.5))/d\sigma(\gamma) \simeq 5 \times 10^3 .$$

Folding in the experimental resolution $\Delta m \simeq 0.5$ GeV, the apparent peak to background ratio would be reduced to 1300, which is over two orders of

magnitude above the measured $\Upsilon(9.5)$ signal.[20] Thus a $Z_3(9.5)$ interpretation of the Υ enhancement is out of the question. Further, the absence of any hundred-fold enhancements above background for lepton-pair masses up to 15 GeV rules out any light Z_3 in this mass range, or close above.

We estimate the Drell-Yan cross sections in the framework of the scaling parton model, taking the valence quark distributions from Ref. 19 and and adjusting the sea quark distribution to reproduce the latest Columbia–Fermilab–Stony Brook (CFS) results[20] for $pA \rightarrow \mu^+\mu^-X$ at 400 GeV on heavy targets. This requires a sea distribution $\bar{u}(x) = \bar{d}(x) = 0.51(1 - x)^{10}/x$. The solid curve in Fig. 9 shows the resulting fit to the 400-GeV CFS continuum data, outside the $\Upsilon(9.5)$ region, with no Z contributions. Other curves illustrate the effect of a Z_3 of mass 16, 18, or 20 GeV. The tail of such a resonance elevates the cross section somewhat in the 10–15 GeV range; The present data seem to exclude a Z_3 mass less than 18 GeV. The extrapolation of the continuum background beyond the measured range depends sensitively on the assumed x dependence of quark distributions; however, the height of the Z_3 peak above background is independent of the sea distribution.

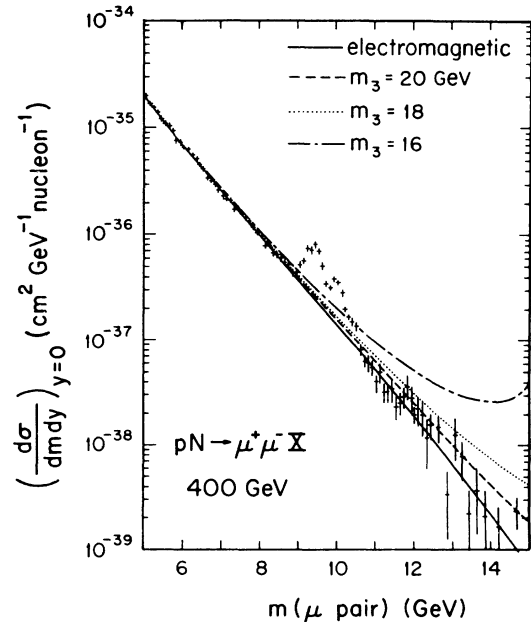Figure 10 shows Drell-Yan predictions for 30-GeV-on-GeV pp colliding beams, with the

FIG. 9. Muon pair production cross section in proton-nucleus scattering at $E = 400$ GeV, $y = 0$. The curves are based on a scaling parton model. The solid curve represents purely electromagnetic scattering, the other curves show the effects of Z_3 (dashed $m_3 = 20$ GeV, dotted $m_3 = 18$ GeV, dash-dotted $m_3 = 16$ GeV). The predictions are based on $\sin^2\theta = 0.6$. Data are from Ref. 20.
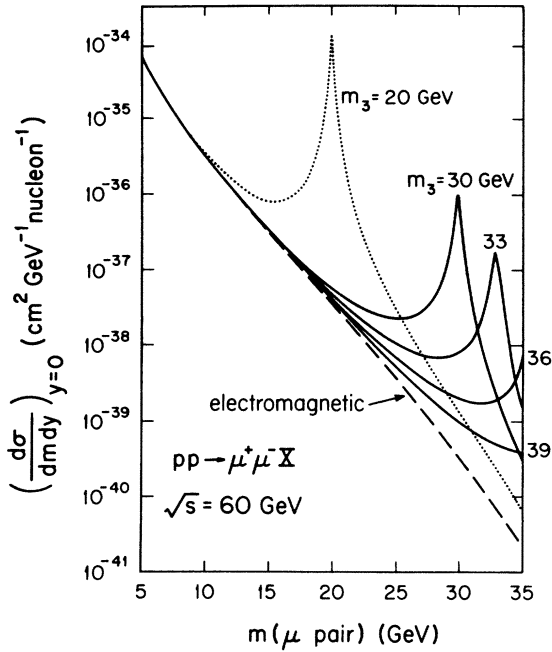
FIG. 10. Drell-Yan predictions for muon pair production by 30-GeV-on-30-GeV pp colliding beams.

cases $m_3 = 20$, 30, 33, 36, and 39 GeV. It is interesting to compare the integral over the Z_3 peak above background with that of the $\Upsilon(9.5)$, since this is a rough measure of the relative counting rates. For this we assume that Υ production scales with the continuum and thus can be estimated using the Fermilab data.[20] We find

$$\frac{\int \sigma(Z_3)\,dm}{\int \sigma(\Upsilon)\,dm} \approx 10, \quad \text{for } m_3 = 20 \text{ GeV}$$

$$\approx 0.1, \quad \text{for } m_3 = 30 \text{ GeV} \qquad (44)$$

for 30-GeV-on-30-GeV pp colliding beams. ISR experiments in progress should detect such a Z_3 signal if it exists.

Figure 11 shows Drell-Yan predictions for 400-GeV-on-400-GeV pp and $\bar{p}p$ colliding beams, as planned for ISABELLE and CERN. The case $m_3 = 30$ GeV is illustrated. Both the Z_1 and Z_2 couplings to the $\mu^+\mu^-$ channel are suppressed, for this case.

Nonscaling corrections to the Drell-Yan formula may change our cross-section extrapolations above Fermilab energies. However, the peak-to-background ratios should remain essentially the same.

E. Deep-inelastic neutral-current scattering

In $\mu^\pm N \to \mu^\pm X$ deep-inelastic scattering, a light Z_3(axial) boson exchange introduces nonscaling effects and differences between μ^+ and μ^- cross sections. The photon-Z_3 interference modification of the deep-inelastic cross section based on the parton model enters through the F_3 structure function

$$\frac{d^2\sigma(\mu^\pm)}{dx\,dy} = \frac{4\pi\alpha^2 ME}{Q^4}\left\{[1 + (1-y)^2]\,xF_1\right.$$

$$\left.\pm[1 - (1-y)^2]\,xF_3\right\}, \qquad (45)$$
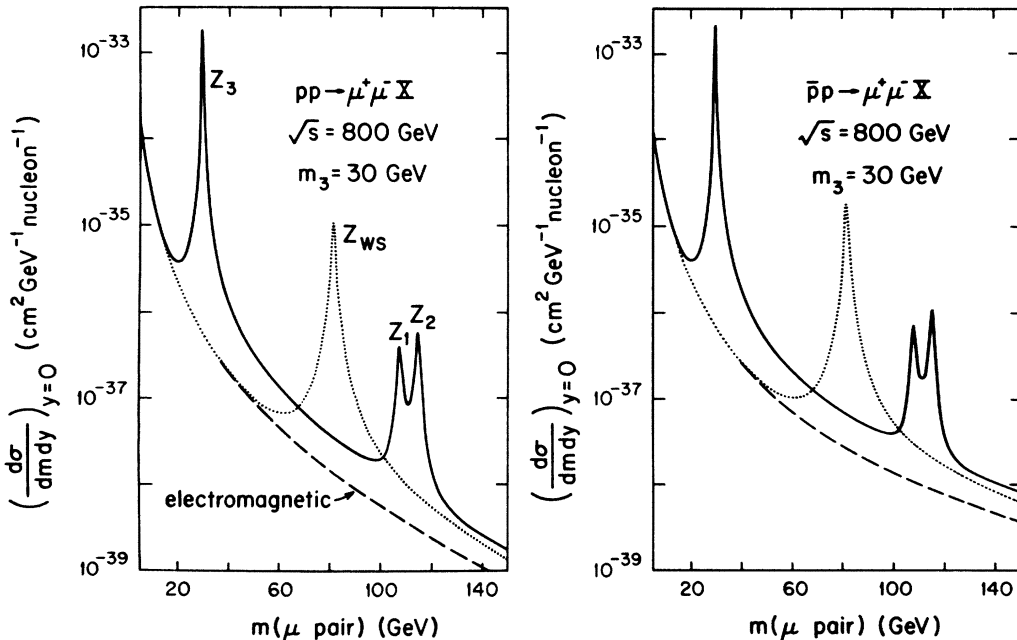
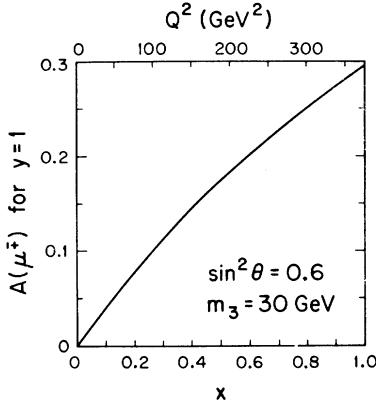FIG. 11. Drell-Yan predictions for muon pair production by 400-GeV-on-400-GeV pp and $\bar{p}p$ colliding beams.

FIG. 12. The asymmetry $A(\mu^{\mp}) = [d\sigma(\mu^-) - d\sigma(\mu^+)]/[d\sigma(\mu^-) + d\sigma(\mu^+)]$ in $\mu N \to \mu X$ deep-inelastic scattering at $E = 200$ GeV, $y = 1$, shown vs x (or Q^2). A Z_3 mass of 30 GeV is assumed.

where the structure functions are the sums of scaling parton densities

$$F_1 = \sum_k e_k^2 f_k(x),$$

$$F_3 = \sum_k e_k H_A^q G_A^\mu f_k(x),$$
(46)

and e_k is the quark charge in units of e. The weak coefficients are

$$H_A^q G_A^\mu = \frac{g_{A3}^q g_{A3}^\mu}{4\sin^2\theta} \frac{Q^2}{Q^2 + m_3^2},$$
(47)

with the g_A given in Eq. (29) and q denoting the quark q_k.

The $\mu^{\pm}$ asymmetry

$$A(\mu^{\mp}) \equiv \frac{d\sigma(\mu^-) - d\sigma(\mu^+)}{d\sigma(\mu^-) + d\sigma(\mu^+)}$$
(48)

vanishes at $y = 0$ and also at $x = 0$, because the sea contributions to F_3 cancel. It is maximal at $y = 1$, for any given x. Figure 12 illustrates the expected x dependence of the asymmetry at $E = 200$ GeV and $y = 1$, for a Z_3 mass of 30 GeV, with $\sin^2\theta = 0.6$ as usual, using the quark distributions from Ref. 19.

The neutral-current interaction of neutrinos with quarks is transmitted by three Z bosons with different masses, whose propagators introduce scalebreaking in addition to any scalebreaking in the quark distributions. In particular, a light Z_3 mass may cause observable nonscaling effects in its contributions to the cross section.

F. Muon anomalous magnetic moment

The weak contributions to $a_\mu = \frac{1}{2}(g_\mu - 2)$ from triangle diagrams is [21]
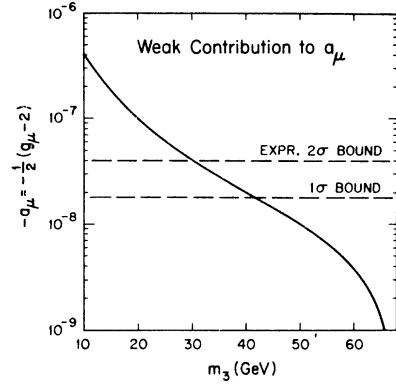
FIG. 13. Weak contribution to the muon anomalous magnetic moment $a_\mu = \frac{1}{2}(g_\mu - 2)$ vs m_3. The experimental 1σ and 2σ bounds on this quantity are shown.

$$a_\mu = \frac{G_F m_\mu^2}{12\sqrt{2}\,\pi^2}\left(5 + \sum_i \frac{m_W^2}{m_i^2}\left[(g_{Vi}^\mu)^2 - 5(g_{Ai}^\mu)^2\right]\right),$$
(49)

where the first term on the right-hand side comes from $W^{\pm}$ and the summation refers to the three bosons Z_i. The result for a_μ with $\sin^2\theta = 0.6$ is plotted vs m_3 in Fig. 13. The discrepancy between the latest experimental value[22] for a_μ and the theoretical electromagnetic contributions through eighth order[23] is

$$a_\mu(\exp) - a_\mu(\mathrm{em}) = (4 \pm 22) \times 10^{-9}.$$
(50)

This sets a limit on the acceptable size of weak contributions. In Fig. 13 the 1σ and 2σ bounds from Eq. (50) are shown; the 2σ bound requires

$$m_3 \geq 30 \text{ GeV}.$$
(51)

This is the most stringent bound we have encountered, for $V^2 + 2A^2$ models. (After submitting this paper for publication, we received a report from Leveille[24] in which similar conclusions about limits on the Z_3 mass are obtained from the a_μ measurements.)

[1]J. C. Pati and A. Salam, Phys. Rev. D **8**, 1240 (1973): **10**, 275 (1974).

[2]R. N. Mohapatra and J. C. Pati, Phys. Rev. D **11**, 566, (1975); **11**, 2558 (1975).

[3]G. Senjanovic and R. N. Mohapatra, Phys. Rev. D **12**, 1502 (1975); R. N. Mohapatra and G. Senjanovic, Phys. Lett. **73B**, 176 (1978).

[4]J. C. Pati, S. Rajpoot, and A. Salam, Phys. Rev. D **17**, 131 (1978); Phys. Lett. **71B**, 387 (1977); H. S. Mani *et al., ibid.* **72B**, 75 (1977).

[5]H. Fritzsch and P. Minkowski, Nucl. Phys. **B103**, 61 (1976).

[6]R. N. Mohapatra and D. P. Sidhu, Phys. Rev. Lett. 38, 667 (1977); Phys. Rev. D **16**, 2843 (1977); 18, 856 (1978).

[7]A. De Rújula, H. Georgi, and S. L. Glashow, Ann. Phys. (N.Y.) **109**, 242 (1977); **109**, 258 (1977).

[8]M. A. B. Bég *et al.*, Phys. Rev. Lett. **39**, 1054 (1977).

[9]E. Ma, Phys. Lett. **73B**, 49 (1978); E. Ma and S. Pakvasa, Phys. Rev. D **17**, 1881 (1978).

[10]R. N. Mohapatra, F. E. Paige, and D. P. Sidhu, Phys. Rev. D **17**, 2462 (1978).

[11]P. Langacker and D. P. Sidhu, Phys. Lett. **74B**, 233 (1978).

[12]V. Elias, J. C. Pati, and A. Salam, Phys. Lett 73B, 451 (1978); V. Elias, Phys. Rev. D **16**, 2284 (1977).

[13]Q. Shafi and C. Wetterich, Phys. Lett. **73B**, 65 (1978).

[14]E. N. Fortson *et al.*, Nature (Lond.) **264**, 528 (1976).

[15]Other gauge models suppressing atomic parity violation, based on an $SU(2) \times U(1) \times U(1)$ symmetry, have been discussed by G. G. Ross and T. Weiler, Caltech Report No. CALT-68-620, 1977 (unpublished); D. Darby and G. Grammer, Illinois Report No. TH-77-39 (unpublished); K. Inoue *et al.*, Prog. Theor. Phys. **58**, 1914 (1977).

[16]H. Georgi and S. Weinberg, Phys. Rev. D **17**, 275 (1978).

[17]See for example, A. McDonald, Nucl. Phys. **B75**, 343 (1974); R. Budny, Phys. Lett. **55B**, 227 (1975); M. Perrottet, Harvard Report No. HUTP-77/AO48 (unpublished).

[18]S. D. Drell and T. M. Yan, Phys. Rev. Lett. **25**, 316 (1970).

[19]V. Barger and R. J. N. Phillips, Nucl. Phys. **B73**, 269 (1974).

[20]D. M. Kaplan *et al.*, Phys. Rev. Lett. **40**, 435 (1978).

[21]See for example, D. Darby and G. Grammer, Nucl. Phys. **B111**, 56 (1976).

[22]J. Bailey *et al.*, Phys. Lett. **67B**, 225 (1977).

[23]J. Calmet *et al.*, Rev. Mod. Phys. **49**, 21 (1976).

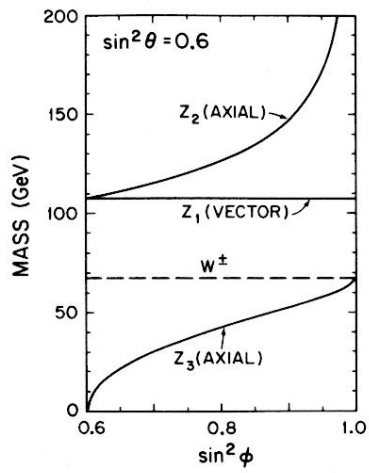[24]J. P. Leveille, Imperial College Report No. ICTP/77-78/2 (unpublished).

FIG. 1. Dependence of the Z masses on the parameter ϕ, for the choice $\sin^2\theta = 0.6$.
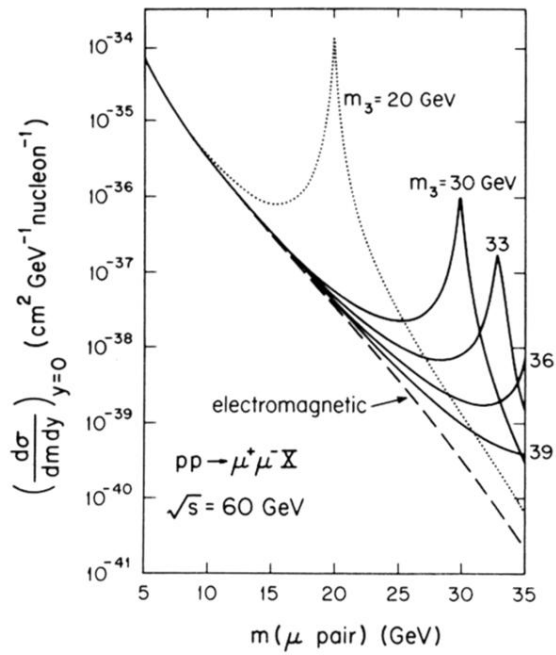
FIG. 10. Drell-Yan predictions for muon pair production by 30-GeV-on-30-GeV pp colliding beams.
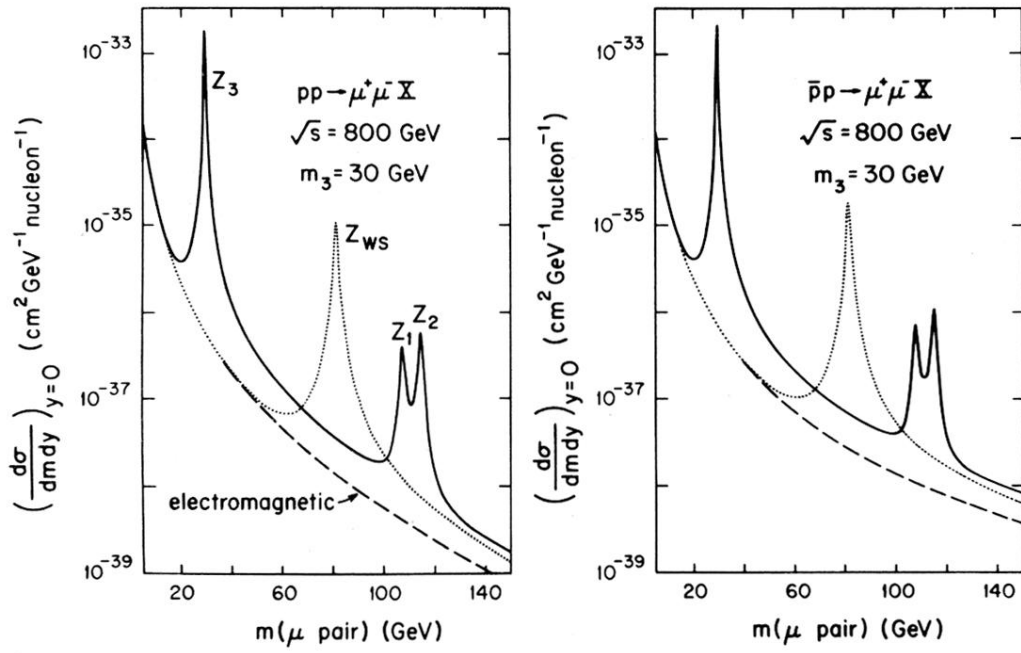
FIG. 11. Drell-Yan predictions for muon pair production by 400-GeV-on-400-GeV pp and $\bar{p}p$ colliding beams.
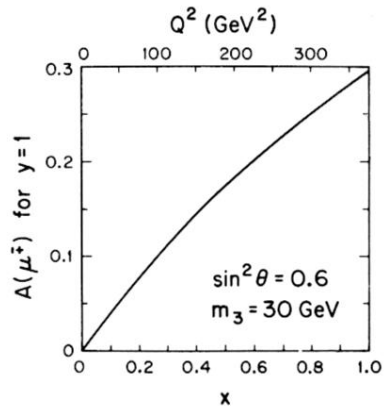
FIG. 12. The asymmetry $A(\mu^{\mp}) = [d\sigma(\mu^-) - d\sigma(\mu^+)]/$ $[d\sigma(\mu^-) + d\sigma(\mu^+)]$ in $\mu N \to \mu X$ deep-inelastic scattering at $E = 200$ GeV, $y = 1$, shown vs x (or Q^2). A Z_3 mass of 30 GeV is assumed.
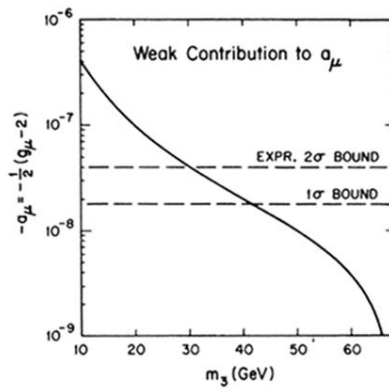
FIG. 13. Weak contribution to the muon anomalous magnetic moment $a_\mu = \frac{1}{2}(g_\mu - 2)$ vs m_3. The experimental 1σ and 2σ bounds on this quantity are shown.
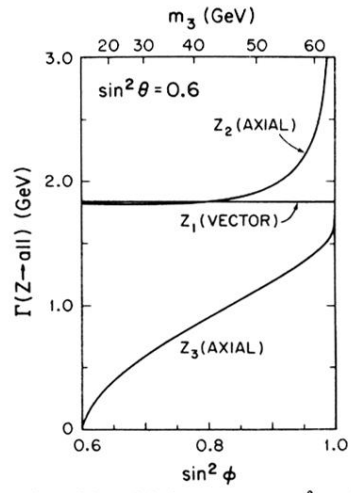
FIG. 2. Total widths of Z bosons vs $\sin^2\phi$, for $\sin^2\theta = 0.6$.
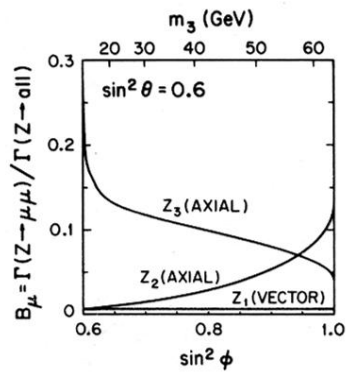
FIG. 3. Branching fractions for $Z \to \mu^+\mu^-$ vs $\sin^2\phi$, for $\sin^2\theta = 0.6$. The branching fraction for Z_1 is 0.006.
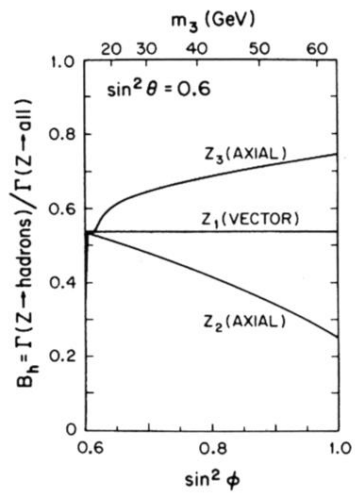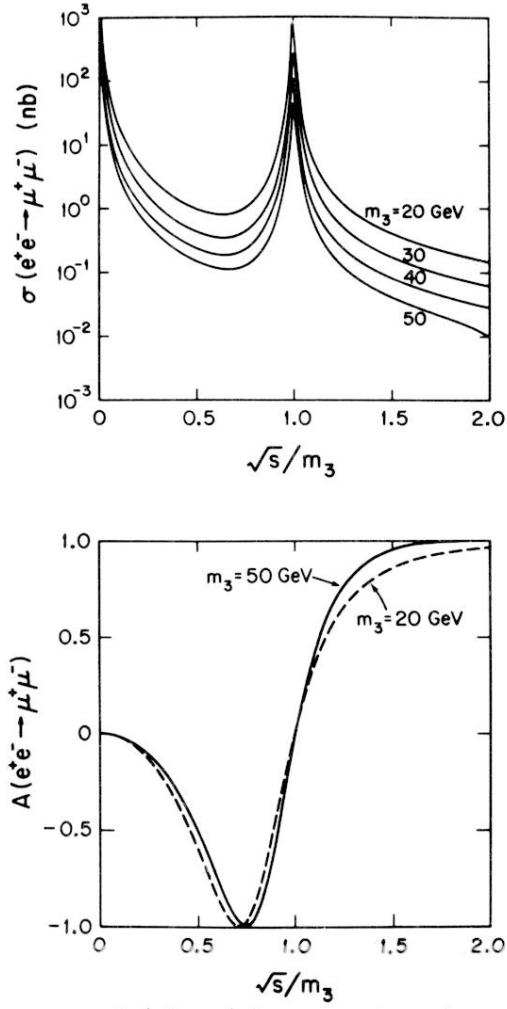
FIG. 4. Branching fractions for $Z \to$ hadrons.

FIG. 5. Total $e^+e^- \to \mu^+\mu^-$ cross section and asymmetry parameter $A(z = 1)$ vs $\sqrt{s}/m_3$. The cases shown have $\sin^2\phi = 0.64$, 0.70, 0.78, 0.88 (with $\sin^2\theta = 0.6$) corresponding to $m_3 = 20$, 30, 40, 50 GeV.
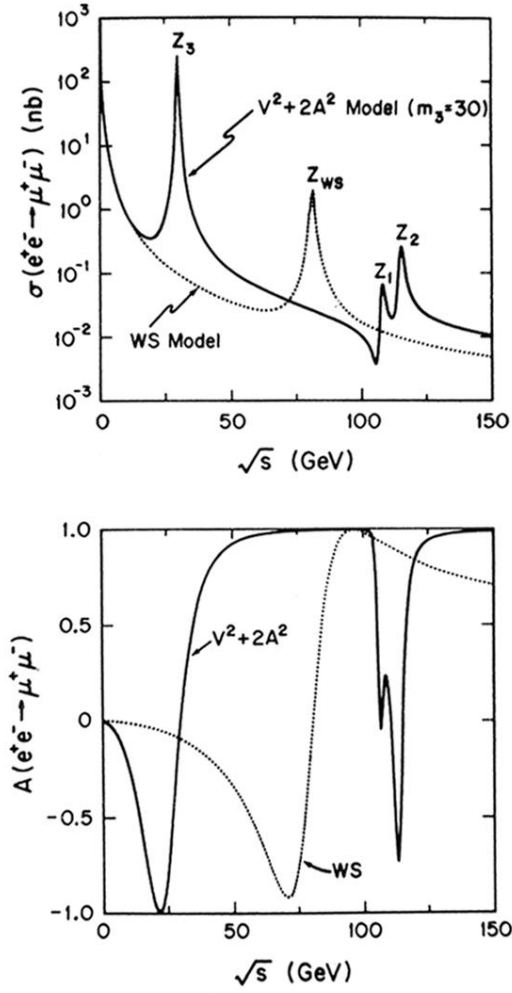
FIG. 6. Total $e^+e^- \to \mu^+\mu^-$ cross section and asymmetry parameter $A(z=1)$, vs $\sqrt{s}$ for $m_3 = 30$ GeV. The WS-model prediction is shown for comparison.

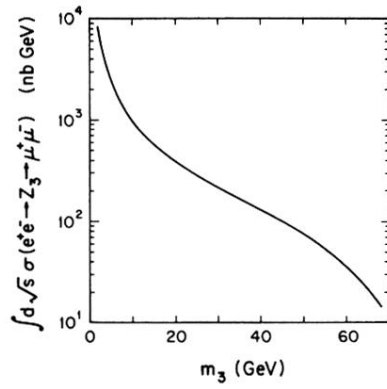FIG. 7. Integrated Z_3 resonance contribution $\int d\sqrt{s}\ \delta(e^+e^- \to Z_3 \to \mu^+\mu^-)$ vs the mass m_3.
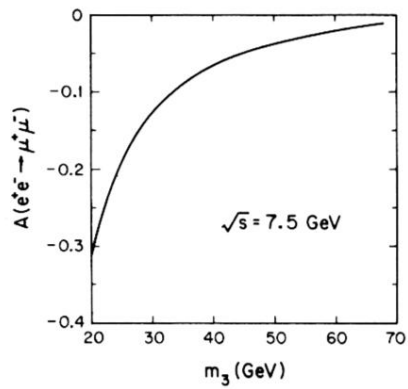
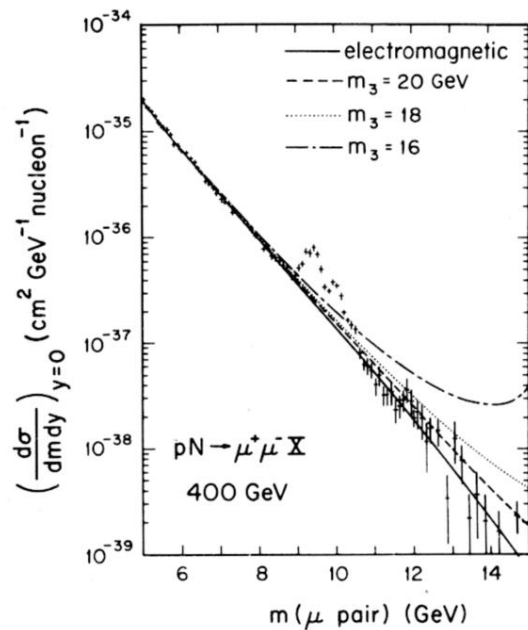FIG. 8. Asymmetry parameter $A\,(z = 1)$ vs m_3 at $\sqrt{s} = 7.5$ GeV.

FIG. 9. Muon pair production cross section in proton-nucleus scattering at $E = 400$ GeV, $y = 0$. The curves are based on a scaling parton model. The solid curve represents purely electromagnetic scattering, the other curves show the effects of Z_3 (dashed $m_3 = 20$ GeV, dotted $m_3 = 18$ GeV, dash-dotted $m_3 = 16$ GeV). The predictions are based on $\sin^2\theta = 0.6$. Data are from Ref. 20.